Hawkmoth flight in the unsteady wakes of flowers

Megan Matthews[1] and Simon Sponberg[1,2]

[1] School of Physics, Georgia Institute of Technology, Atlanta, GA
[2] School of Biological Sciences, Georgia Institute of Technology, Atlanta, GA

correspondence: mmatthews36@gatech.edu

Abstract

Flying animals maneuver and hover through environments where wind gusts and flower wakes produce unsteady flow. Although both flight maneuvers and aerodynamic mechanisms have been studied independently, little is known about how these interact in an environment where flow is already unsteady. Moths forage from flowers by hovering in the flower's wake. We investigate hawkmoths tracking a 3D-printed robotic flower in a wind tunnel. We visualize the flow in the wake and around the wings and compare tracking performance to previous experiments in a still air flight chamber. Like in still air, moths flying in the flower wake exhibit near perfect tracking at low frequencies where natural flowers move. However, tracking in the flower wake results in a larger overshoot between 2-5 Hz. Smoke visualization of the flower wake shows that the dominant vortex shedding corresponds to the same frequency band as the increased overshoot. Despite these large effects on tracking dynamics in wind, the leading edge vortex (LEV) remains bound to the wing throughout the wingstroke. The LEV not only persists in the flower wake, but also maintains the same qualitative structure seen in steady air. Persistence of a stable LEV during decreased flower tracking demonstrates the interplay between hovering and maneuvering.

Keywords: *Manduca sexta*, flight, flower tracking, leading edge vortex, unsteady flow, system identification.

Introduction

Flying animals rely on maneuverability to survive in unsteady environments whether evading predators, finding mates, or foraging for food (Dudley 2002*b*, Sprayberry & Daniel 2007, Broadhead et al. 2017). As these animals actively move through their environments, locomotion depends on interactions between their body and the surrounding fluid to produce necessary forces and torques. Changing fluid environments naturally manifest unsteady airflow. Animals must respond to perturbations due to wind gusts and wakes shed from flowers and other objects (Sane 2003, Ravi et al. 2015). Successful flight control requires managing the impact of unsteady flow on body maneuvers and aerodynamic forces as well as any emergent interaction effects (Fig. 1).

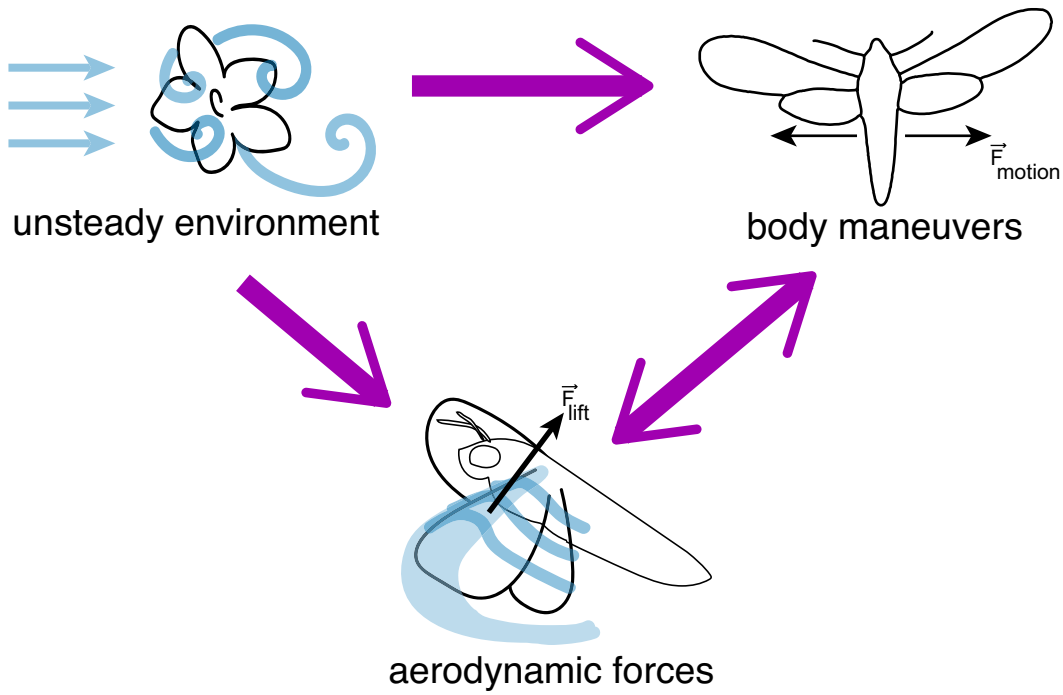

Fig. 1. Components for flight success. Insects flying in natural environments must (often simultaneously) (1) interact with unsteady wind, (2) generate stable lift forces through aerodynamic mechanisms, such as the leading edge vortex (LEV), and (3) perform complex body maneuvers to complete tasks. As aerodynamic forces and body maneuvers are changed interaction effects may emerge, hence the double arrow.

Themes governing how unsteady flow influences flight are elucidated through experiments on stationary (Ortega-Jimenez et al. 2013, Pournazeri et al. 2013, Ortega-Jimenez et al. 2014) or

simplified (Combes & Dudley 2009, Lentink et al. 2010, Ortega-Jimenez et al. 2016, Ravi et al. 2016) flight behaviors. Despite our understanding of complex flight mechanisms in steady air, we still do not know how unsteady flow impacts maneuverability. Nor do we know if fundamental aerodynamic mechanisms present in hovering flight persist when an animal must maneuver in flow that is already unsteady.

Hawkmoths must maneuver in unsteady flow while hovering to feed in the wakes of flowers. They control their distance to the flower as well as quickly responding to environmental perturbations and changes in flower position (Farina et al. 1995, Sprayberry & Daniel 2007, Sprayberry & Suver 2011, Sponberg et al. 2015, Roth et al. 2016). Using precisely coordinated wing and body kinematics (Sponberg & Daniel 2012), the agile hawkmoth *Manduca sexta*, has adapted robust mechanisms to shift the balance between stability and maneuverability depending on the desired behavior (Dudley 2002*a*, Dyhr et al. 2013). Hawkmoths modulate their kinematics to track flower motion up to 14 Hz, well above what they encounter in nature, albeit with poor performance (Sponberg et al. 2015).

Coordinated wing and body kinematics are also responsible for lift production through unsteady aerodynamic mechanisms (Weis-Fogh 1973, Lighthill 1973). One mechanism, the ubiquitous leading edge vortex (LEV), is thought to contribute to the high lift achieved in insect flight (Ellington et al. 1996, Sane 2003, Chin & Lentink 2016). The LEV has been visualized both qualitatively and quantitatively revealing the basic vortex structure, its dynamics throughout a wingstroke, and vortex stabilization for many insect species (Srygley & Thomas 2002, Bomphrey et al. 2005, 2009). However, the LEV has only been visualized in steady flow (Willmott et al. 1997, Willmott & Ellington 1997*a*,*c*,*b*). Moths may need to alter wing motion to maintain lift generation in unsteady flow which could disrupt the quasi-steady LEV. LEV disruption is visualized as vortex bursting, which can occur when increased momentum deflects flow through the vortex core. The deflected flow alters the LEV structure and attachment to the wing (Birch & Dickinson 2001, Lentink & Dickinson 2009). Although we understand how the LEV generates lift, it is not known how vortex structure and stability are affected by flow in the environment that is already unsteady.

For the hawkmoth, unsteady flow is generated in the environment when natural winds encounter flowers. As wind moves around the flower shape, vortices are shed into the wake. Foraging moths feeding from these flowers must interact with these vortices. The unsteady wake can potentially disrupt tracking maneuvers and the structure of the LEV. Changes to LEV structure and lift production could result in changes to body maneuvers and vice versa (Fig. 1). How do flower wake interactions lead to changes in tracking maneuvers? And how does the LEV interact with unsteady flow already in the environment? In order to address these two questions, we must investigate the interplay between maneuvering, aerodynamics (specifically the LEV), and unsteady flow.

To do this we have moths track robotic flowers in a wind tunnel, where we can control the flow environment. In wind, we also visualize the unsteady wake around the robotic flower, natural flowers, and the moth to reveal impacts on the LEV structure.

If flower tracking performance decreases in wind, then moths must balance reactions to unsteady flow (i.e. the flower wake) with foraging maneuvers. In this case, we predict that moths will

react to unsteady flow by matching the dominant vortex shedding frequencies in the flower wake. Consequently, foraging maneuvers used to track the flower will suffer the most at these frequencies.

If the leading edge vortex is disrupted in the flower wake, then we expect to observe LEV growth, and potentially bursting, when the wings interact with vortices in the flower wake. However, if the leading edge vortex maintains the same structure and attachment in the flower wake, then the LEV is a stable lift mechanism in both still and windy environments.

Methods

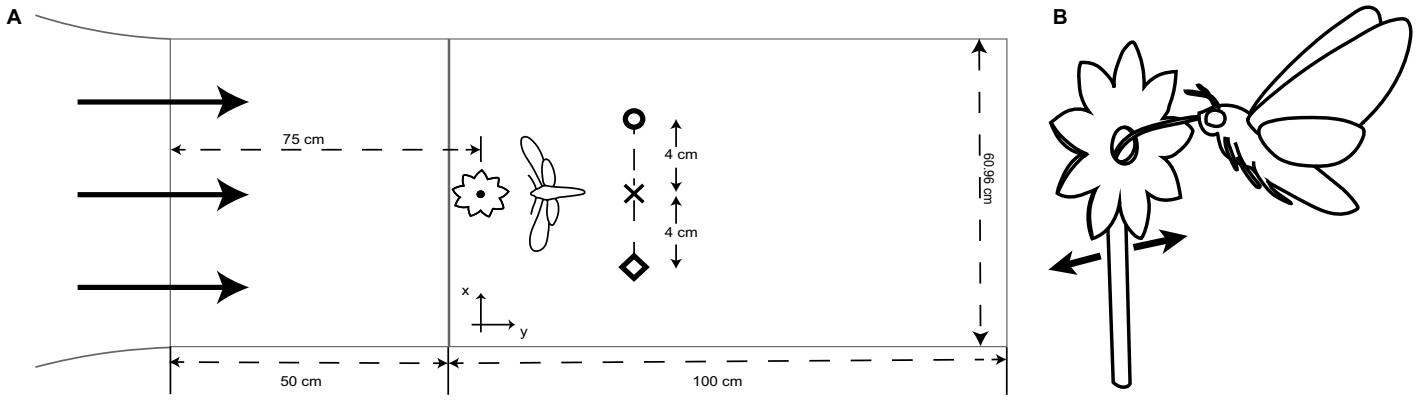

Fig. 2. Experimental set-up and conditions. (A) Schematic diagram of the wind tunnel test section. The robotic flower is placed approximately 75 cm downstream (y-direction) of where flow enters and the moth feeds 2-5 cm downstream of the flower. Wind speed measurements were taken at multiple lateral positions (4 cm apart, marked by symbols) with and without the flower (Fig. S1). (B) Sketch of the hawkmoth feeding from the robotic flower. The moth hovers without landing and tracks as the flower laterally oscillates.

Wind tunnel characteristics

We performed experiments using an open-circuit Eiffel-type wind tunnel (ELD, Inc.). The 150 cm working section consisted of two interchangeable test sections with 60.96 cm symmetric cross-sections (schematic drawing in Fig. 2A). The fan is driven by a 3HP induction motor (belt-driven, ODP, 208/230VAC) and generates continuously variable wind speeds from 0.25 - 10 m s^{-1} with less than ±2% variation of the mean. See supplement for specific component details and specifications.

Flow characteristics

We placed a 3D-printed robotic flower (Sponberg et al. 2015) at the front of the secondary test section, 75-80 cm downstream from the upstream mesh and at the approximate lateral midpoint (Fig. 2A, x symbol). The flower is actuated by a bipolar stepper motor (57STH56 NEMA23 with 1067 controller; Phidgets, Inc.) using a 14.5 cm moment arm and the center of the flower face is 20 cm above the bottom panel of the test section.

Wind speed measurements were made at multiple points along the centerline of the working section using an air velocity transducer (TSI Alnor) both with and without the robotic flower present. Measurements were taken at seven downstream points and three lateral positions (Figs. 2A,S1B).

Experimental set-up and procedure

Moths

The hawkmoths used were shipped as pupae from a colony maintained at the University of Washington on a diet that contains retinoic acid (Sponberg et al. 2015). Prior to experiments, the moths were kept on a 12:12 day:night cycle with foraging/feeding time ("dusk") set around noon EST. Tracking experiments were performed with 5 male and 5 female moths (m=1.87 ± 0.54 g, mean ± s.d.) and still flower experiments with 5 male and 5 female moths (m=1.70 ± 0.32 g, mean ± s.d.); each moth was only used for a single trial, 2-5 days post-ecolsion, and was not exposed to the artificial flower prior to the experiments. For all trials, naïve moths were dark-adapted to the experiment room for a minimum of 30 minutes. Temperature during experiments was maintained between 24-26°C. A seven-component flower scent (mimicking *Datura wrightii*) is applied to the robotic flower to encourage foraging behavior (Riffell et al. 2014).

Prior to experiments, moths were marked with a dot of white paint (1:1 ratio of tempera and acrylic paint) on the ventral side of the thorax for tracking. Only the thorax point was used since head tracking is not significantly different (Stöckl et al. 2017). Once the moth was feeding (and the proboscis was in the nectary, Fig. 2B), we started the flower motion and recorded the positions of both the moth and flower throughout the 20 second tracking run. Moths were removed from the flight chamber if feeding was not initiated within 5 minutes.

Robotic flower

The robotic flower consists of a 3D-printed flower face (5 cm tip-to-tip diameter) and 2 mL glass nectary attached to the stepper motor. Flower motion is prescribed as a sum of 20 sinusoids, each

with a different driving frequency and randomized phase, and controlled through MATLAB. The stimulus is designed to broadly sample the frequency range and minimize potential learning effects (Roth et al. 2011). To limit challenges in analyzing the frequency response, the prescribed driving frequencies are logarithmically-spaced prime multiples (0.2-19.9 Hz) (Roth et al. 2011, Dyhr et al. 2013, Roth et al. 2014). This eliminates ambiguity between whether measured responses are true reactions to the stimulus or a result of harmonic overlap. The velocity of a constant amplitude sinusoidal motion increases linearly with frequency, which may cause moths to reach the saturation limit of their muscle output at the higher frequencies. To avoid this issue, the velocity amplitude of the flower motion is scaled to be constant at all frequencies (Roth et al. 2014).

Video recordings

We recorded all flights from below (ventral view) using a Photron UX100 with a 50 mm lens operating at 125 frames per second (fps). Moths were illuminated with two 850 nm IR lights (Larson Electronics) as well as a "moon light" (Neewer CW-126) used to make the flower face visible and set background luminance (Sponberg et al. 2015). Color temperature, based on a blackbody radiation spectrum, was 5400 K. The moon light was equipped with neutral density filters to reduce the measured illuminance to approximately 0.3 lx (measured in front and to each side of the flower face) for all trials, which is the preferred foraging light level for *M. sexta* (Theobald et al. 2009).

For smoke-wire visualization an additional Photron UX100 (50 mm lens, 125 fps) was used to record the side view of the animal. The ventral view was used to confirm the horizontal position of the smoke plane relative to either the wingspan or the flower. Additionally, the moon light was increased approximately 0.1 lx to enhance smoke visibility in the ventral camera.

Smoke-wire visualization

Smoke visualization (Merzkirch 1987) was performed with a nickel chromium (nichrome) wire aligned with the center of the flower face and approximately 10-20 cm upstream. The 0.25 mm wire was double-coiled and coated with Protosmoke train smoke oil (MTH Trains). After running a current through the wire, the oil condenses into droplets along the length of the wire which are then vaporized into smoke trails as the wire is heated.

Data analysis

Frequency response and tracking performance

After digitizing the flower and moth motions using DLT tracking software (Hedrick 2008), the individual time series were Fourier transformed to be analyzed in the frequency domain (in MATLAB). We can characterize the broad frequency response of the system by the gain and phase, (G, ϕ), at each unique driving frequency (Fig. 3D,E insets). Details of how gain and phase are calculated are given in the supplement.

Tracking error

Instead of separating the real and imaginary components of the frequency response, we can also use the distance from perfect tracking, (1,0), in the complex plane (Fig. 3F, inset) to assess tracking performance (Roth et al. 2011, Sponberg et al. 2015).

$$\varepsilon = \|(1 + 0i) - (G + \phi i)\| \tag{1}$$

For perfect tracking, tracking error should be minimized. Due to the periodic nature of the phase response, tracking error above 1 indicates that the moth would achieve better performance by remaining stationary at that frequency. However, since gain (G) and phase (ϕ) represent full system dynamics over all frequencies it may not be physically possible for the moth to be motionless at any single frequency.

Mechanical (and inertial) power

Interacting with the unsteady flower wake could alter mechanical power requirements compared to tracking in still air. Total mechanical power in insect flight combines contributions from multiple sources including profile and induced power, which refer to drag effects on the wings, and parasite and inertial power, corresponding to body drag and acceleration effects (Dudley 2002*a*). While inertial power contains costs for accelerating the wing mass (and added mass), it also includes costs due to accelerations of the body (center of mass, COM) required for flight maneuvers, such as tracking.

To assess how body maneuvers specific to flower tracking change due to wind, we restrict our analysis to inertial COM mechanical power. Following previous methods (Sprayberry & Daniel 2007), we calculate the inertial power required to laterally accelerate the center of mass during flower tracking. The moth's response to the sum of sinusoid motion of the robotic flower can be written as

$$x\left(t\right) = \sum_{k=1}^{20} A_k \sin\left(2\pi f_k t + \phi_k\right) \tag{2}$$

where the indices k correspond to the 20 driving frequencies. Inertial power (changes in kinetic energy) due to center of mass oscillations is given by

$$\dot{E} = ma\left(t\right) v\left(t\right) \tag{3}$$

with

$$
\begin{aligned}
v(t) &= 2\pi \sum_k (f_k A_k) \cos(2\pi f_k t + \phi_k) \\
a(t) &= -(2\pi)^2 \sum_k \left(f_k^2 A_k\right) \sin(2\pi f_k t + \phi_k)
\end{aligned}
\tag{4}
$$

using the transformations described above. So, the inertial power needed for tracking becomes

$$
\dot{E} = m(2\pi)^3 \sum_k f_k^3 A_k^2 \sin(2\pi f_k t + \phi_k) \cos(2\pi f_k t + \phi_k) \tag{5}
$$

after taking the absolute value. This can be evaluated at each driving frequency and averaged over a quarter cycle giving

$$
\begin{aligned}
\dot{E} &= (4f_k)\left[m(2\pi)^3 f_k^3 A_k^2\right] \int_0^{1/4f_k} \quad \sin(2\pi f_k t + \phi)\cos(2\pi f_k t + \phi) \quad dt \\
\dot{E} &= 8m\pi^2 \sum_k f_k^3 A_k^2.
\end{aligned}
\tag{6}
$$

We restrict our inertial power analysis to only the lateral (horizontal) axis and assume that fluctuations along the vertical and looming axes are relatively constant. Previous experiments with horizontal flower motion showed that downstream distance from the flower (looming axis) and hovering position (vertical axis) remained fairly constant during tracking, which supports our assumptions (Sprayberry & Daniel 2007). Additionally, the magnitude of the (inertial) power required for center of mass oscillations is much smaller than the magnitude of the (aerodynamic) power required for hovering. By comparing the inertial COM power for tracking in wind and still air, we can reveal how flower wake interactions affect body maneuvers.

Statistics

Statistically significant tracking was assessed at each driving frequency using a coherence threshold (Roth et al. 2011, 2014) and Fisher's exact g test for periodicity (± 0.5 Hz frequency bands around each driving frequency were tested with a confidence threshold of 0.05 (Sponberg et al. 2015)). Additionally, all averaging and variance estimation were performed in the complex plane (Roth et al. 2011). These values were comparable to results for averaging log gain and using circular statistics to average phase (Roth et al. 2016). Error bars are 95% confidence intervals of the mean unless otherwise noted.

Gain, phase, and tracking error were all tested for significance using parametric, two-factor ANOVA (with wind and frequency as our factors). This test was also used to determine significant differences in inertial power within specific frequency bands.

Results

Tracking performance decreases in an unsteady flower wake

In unsteady air, all moths successfully tracked for the full 20 seconds with significant tracking at least up to 6.1 Hz with 0.90 coherence (Roth et al. 2011, Sponberg et al. 2015) (Fig. 3B, gray line). Most moths (70%) were able to significantly track up to 11.3 Hz, but few moths (30% or less) were able to track any higher frequencies. This is lower than in still air, where half of the moths significantly tracked flower motion up to 13.7 Hz.

Comparisons between the frequency responses for tracking in wind and still air are best interpreted by examining specific frequency bands: (i) 0.2-1.7 Hz, (ii) 1.7-5.3 Hz, and (iii) 5.3-11.3 Hz. The first band corresponds to the range at which natural hawkmoth-pollinated flowers oscillate (Sponberg et al. 2015, Stöckl et al. 2017), the second captures the range with the largest overshoot in position (Fig. 3B), and the third describes how the moths modulate tracking as they fail.

(i) Low frequency response: Moths track best at natural flower oscillation frequencies

When tracking in wind, moths interact with unsteady flow in the roboflower's wake, but the effect of these interactions on moth dynamics is very small at the lowest frequencies. Even in wind, moths track nearly perfectly ($G = 1; \phi = 0$) across low frequencies up to 0.7 Hz, revealing only minor difference with tracking in still air (gain and phase difference at 0.7 Hz: 0.15 and 2.8°, Fig. 3D,E). Across all low frequencies, 0.2-1.7 Hz, the moth's gain was higher in windy conditions than in still air, increasing by 14% at 1.7 Hz (gain for 0.2-1.7 Hz: $F=30.25$, $dF=1$, $P<0.05$). However, there were no distinguishable differences in the phase response (0.2-1.7 Hz: $F=0.6$, $dF=1$, $P=0.4393$).

Higher gain does not necessarily indicate improved tracking performance. Because the moth was overshooting the flower in windy conditions, the tracking error was larger than in still air (0.7-1.7 Hz, $F=11.14$, $dF=1$, $P=0.0012$, Fig. 3F, blue line). However error is still below 1 until the end of this frequency band (1.11 ± 0.09 at 1.7 Hz), showing that maneuvers do still produce a net tracking benefit.

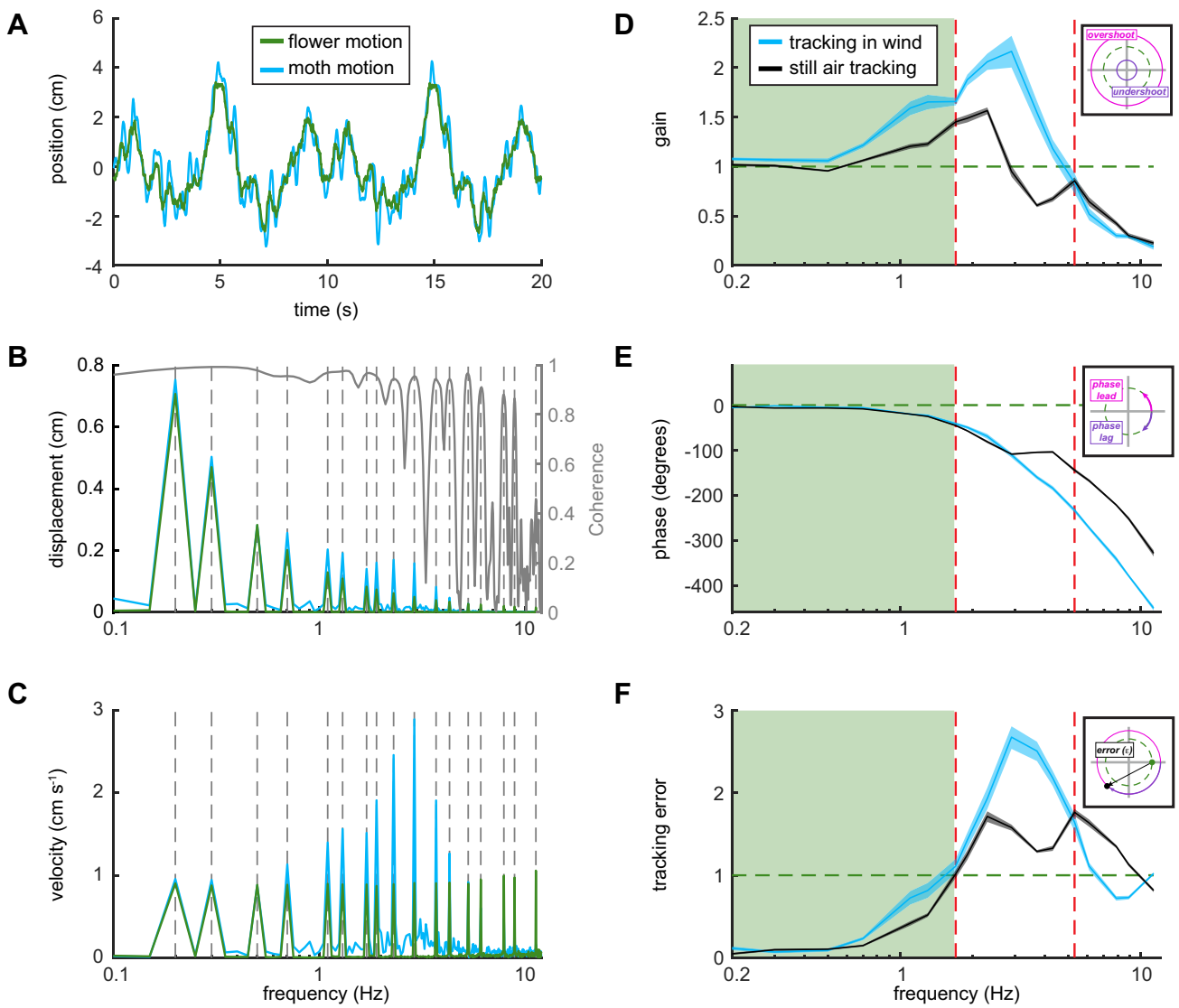

Fig. 3. Frequency response comparison for tracking with and without wind. All still air data (black) previously collected in Sponberg et al (2015). (A) Example raw time series data for one trial of tracking in wind. The moth (blue) overshoots the flower (green) throughout the trial. (B) (left axis) Amplitude (position) in the frequency domain (after Fourier transform of data from A). Peaks correspond to prescribed flower driving frequencies. (right axis) Coherence threshold shows significant tracking drops below 0.9 above 6 Hz. (C) Velocity in the frequency domain. Despite the flower velocity scaled to be equal in amplitude at each driving frequency, moths show large variations at mid-range frequencies. (D, E) Frequency responses (mean ± 95% CI of the mean) for the same tracking task in still (black) and unsteady (blue) air. Responses are categorized into three frequency bands, separated by (red) dashed lines at 1.7 Hz and 5.3 Hz. Gain (D) describes the relative amplitude difference between moth and flower while phase (E) characterizes timing differences. The insets graphically show how gain, phase and tracking error are interpreted in the complex plane. Moths in both conditions show best tracking performance (with perfect tracking at gain=1 and phase=0°) in the frequency band below 1.7 Hz although tracking in wind results in earlier and increased overshoot. (F) Gain and phase are combined and used to calculate tracking error, the distance from perfect tracking in the complex plane. For both conditions, tracking error is minimized in the low-frequency range. The green box denotes the frequency range below 1.7 Hz which matches the range of oscillations exhibited by natural hawkmoth-pollinated flowers.

(ii) Intermediate frequency response: Interaction with wind decreases tracking performance

As in still air, moths tracking in wind have a distinct region of overshoot ($G > 1$) in the intermediate frequency range (Fig. 3D). However overshoot is both more pronounced and persists over a greater range of frequencies in wind (peak $G = 2.17 \pm 0.16$, ϕ =109.9° ± 5.9° at 2.9 Hz). Overall, tracking in wind between 1.7-5.3 Hz results in a nearly 40% higher peak overshoot (gain: *F=79.52, dF=1, P<0.05*). Tracking in wind also removes the plateau in the phase response, producing a monotonic roll off not seen in still air (phase: *F=5.57, dF=1, P=0.0201*).

Tracking error throughout this frequency band is large due to a combination of gains above 1 and phase lags greater than 90°. Maximum tracking error in windy conditions is higher than in still air, with a 70% increase at 2.9 Hz. Tracking error in wind steadily increases until the maximum of 2.68 ± 0.14 at 2.9 Hz (Fig. 3E, blue line) and then decreases until it falls just below the maximum of still air tracking error (1.65 ± 0.11 at 5.3 Hz), resulting in a statistically significant difference with and without wind (*F=58.62, dF=1, P<0.05*). In both cases, but especially with wind, the moth would track these intermediate frequencies better if it stayed stationary ($G = 0; \phi = 0; \epsilon = 1$).

(iii) High frequency response: Moths show similar failure dynamics while tracking with and without wind

Despite the large overshoot in wind at the mid-range frequencies, moths tracking with and without wind fail similarly as flower motion frequency increases towards the saturation limit of the moths' flight system. Although few moths were able to successfully track above 11.3 Hz in wind, the decrease in gain leading up to this frequency is similar to the response in still air, with no significant difference (*F=3.19, dF=1, P=0.0773*). The approximately 90° difference in phase lag between wind and still air grows until exceeding a 100° difference at 11.3 Hz (Fig. 3D,E). Since tracking error is a distance in the complex plane and phases of 0° and ±360° are equivalent, the increased phase lag for tracking in wind reduces tracking error back toward a value of 1. This results in a maximum difference of 0.63 ± 0.03 between tracking in wind and in still air (*F=36.31, dF=1, P<0.05*).

These differences for tracking with and without wind lead to the differences in tracking error (Fig. 3F). In wind and still air, moths fail by undershooting and lagging behind the flower at higher frequencies until, at the highest frequencies, they are effectively non-responsive ($G = 0; \phi = 0$). As tracking gain approaches zero, the tracking error necessarily approaches 1. In other words, the origin ($G = 0; \phi = 0$) is 1 unit away from perfect tracking ($G = 1; \phi = 0$) in the complex plane (Fig S2).

Flower tracking in wind manifests low-order dynamics

Overall, moths display reduced-order dynamics for tracking in wind compared to still air. Although we assume the same underlying dynamical system, the change in the transfer function (frequency response, Fig. 3D,E) suggests that windy conditions simplify tracking maneuvers. The transfer function describing still air tracking includes a simple delay term (Sponberg et al. 2015, Roth et al. 2016, Stöckl et al. 2017) and a minimum of three poles to capture the double peak in gain, but more importantly, the plateau in phase between 3-5 Hz. In wind, the phase plateau

is removed and tracking can be described with only a second-order transfer function. This order reduction suggests that wind acts as an environmental filter to cancel out certain tracking maneuvers.

Dominant vortex shedding frequencies of unsteady flower wakes coincide with specific frequency bands

(i) Roboflower sheds vortices in the intermediate frequency range, matching the frequency band of overshoot

To explore the temporal dynamics of the unsteady flow around the moth we imaged the wake of robotic flower. Using smoke-wire visualization, we observed that the dominant vortex structures in the flower wake are irregular, but mostly within the intermediate frequency band of 1.7 to 5.3 Hz. The vortex shedding frequency was determined by observing the number of vortices (rotating in the same direction) over 300 frames, approximately 5-10 cm downstream of the flower face (Fig. 4A, red box). Averaging across four videos, the vortex shedding frequency from the top petals was 2.16 Hz $\pm$ 0.25 Hz (mean $\pm$ s.d.). Flow around the nectary shed vortices at 0.95 Hz $\pm$ 0.17 Hz (mean $\pm$ s.d.). However, this is a lower bound of the vortex shedding frequency because the flower sheds vortices that rotate in multiple directions with one or more arriving at the same downstream location simultaneously (Movie S1).

While the streaklines had a slight upward drift due to higher temperature than surrounding air, the flower wake structure is distinct from the undisturbed streaklines above the flower. As the wake develops downstream the shed vortex structures interact with one another. Some vortices cluster (multiple vortices, Fig. 4B), appear distinct (single vortex, Fig. 4C), or merge with counter-rotating, neighboring vortices (diffuse streaklines, Fig. 4D). These overlapping vortices (Fig. 4B,D) potentially double the number of vortices, raising the estimated dominant vortex shedding frequency up to 4.33 Hz $\pm$ 0.49 Hz (mean $\pm$ s.d.) from the top petals and 1.90 Hz $\pm$ 0.34 Hz (mean $\pm$ s.d.) from the nectary. While the moth feeds in a relatively low flow region (approximately 5 cm downstream), the wingspan extends past the face of the flower so structures shed from the perimeter interact directly with both wings.

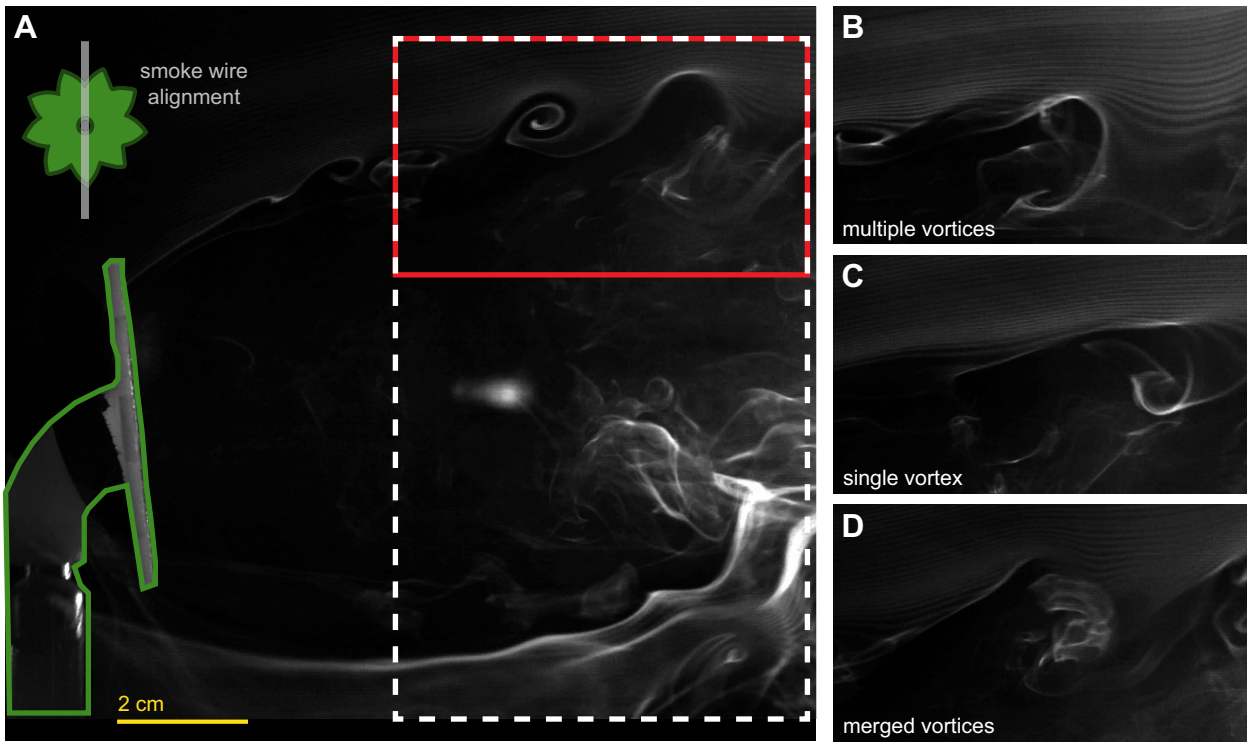

Fig. 4. Smoke visualization of the robotic flower wake. (A) Full frame view of flower wake. Inset shows smoke wire lateral alignment with the flower face. The moth primarily feeds in the relatively low flow region approximately 2-5 cm downstream of the flower. Vortices were most distinguishable around 5 cm downstream (white dashed box) and vortex shedding frequency was measured at this location (red box). (B) Snapshot of flower wake (from red boxed region) showing multiple vortices, rotating in multiple directions, passing through the same location. (C) Snapshot of a single vortex. (D) Snapshot of diffuse streaklines due to merging vortices. Level adjustments were made to highlight the smoke lines using Photoshop with a mask over the robotic flower, shown in green.

(ii) Real hawkmoth-pollinated flowers shed unsteady wakes at low frequencies

Size and material differences between our robotic flower and natural flowers could lead to different unsteady wakes. Hawkmoths forage from flowers of various sizes, from 1-2 cm up to 10 cm (Sprayberry & Suver 2011, Sponberg et al. 2015) and natural flowers are much softer than the 3D-printed roboflower. Using the same visualization method, we observed the wakes shed from fully bloomed *Datura sp.* (tip-to-tip, flower face diameter: 9 cm, Fig. 5A) and *Petunia sp.* flowers (tip-to-tip, flower face diameter: 7 cm, Fig. 5B) attached to the same rigid support used for the robotic flower. Larger *Datura* flowers shed vortices 2-3 cm further downstream than *Petunia*. This includes the feeding position of the moth (Fig. 5A). Fewer vortices appear in the measurement region (Fig. 5, red box) resulting in a lower frequency of structures shed off the flower petals, (lower bound: 0.43 Hz $\pm$ 0.06 Hz; upper bound: 0.87 Hz $\pm$ 0.12 Hz). The vortex shedding frequency around the nectary was similar to the roboflower since the same support structure was used (bottom wake structure, Fig. 5A). Averaging over three *Datura* videos gives a lower bound of 0.88 Hz $\pm$ 0.26 Hz and an upper bound of 1.77 Hz $\pm$ 0.51 Hz. For *Petunia*, these vortices are partially disrupted due

to interactions with the lower set of petals, which did not allow for measurement of vortex shedding in this region (Fig. 5B). Based on three different *Petunia*, and averaged over four videos, the vortex shedding frequency is 0.95 Hz ± 0.18 Hz. Unlike the robotic flower wake, *Petunia* showed fewer overlapping vortices, but vortices were still multi-directional, so while an upper bound of 1.90 Hz ± 0.36 Hz is unlikely, some structures are shed at frequencies above 1 Hz.

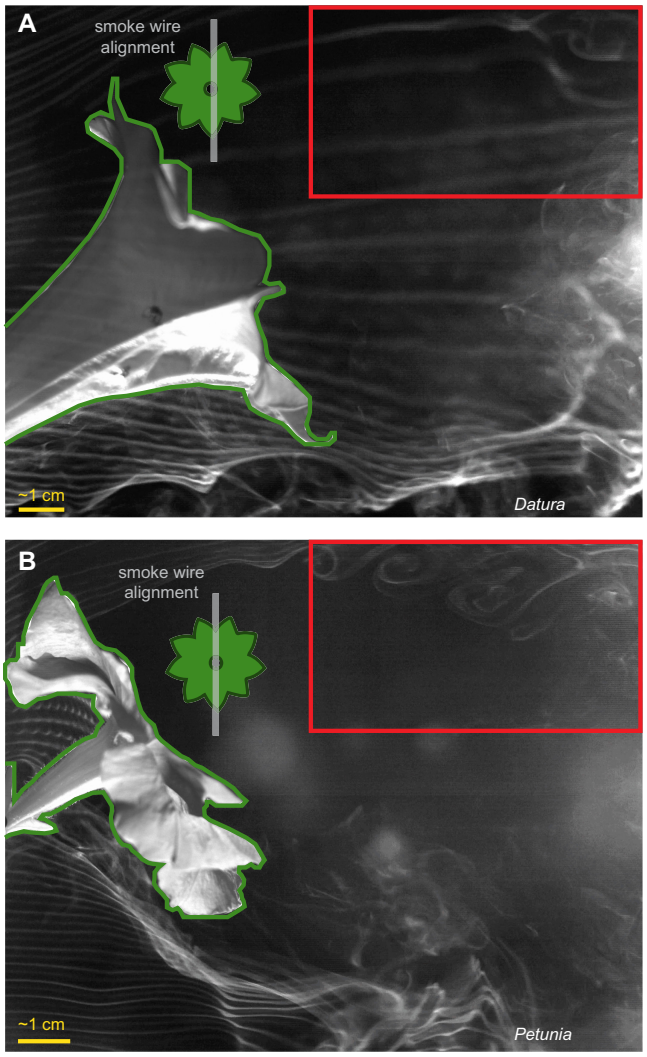

Fig. 5. Smoke visualization of natural flower wakes. (A) Snapshot of *Datura sp.* wake. (B) Snapshot of *Petunia sp.* wake. Inset shows smoke wire lateral alignment with the flower face. For both flowers, vortices similar to those shed by the robotic flower are seen coming from the top petals, with fewer passing through the measurement region for *Datura* (red box). The wake structure from the bottom petals is disrupted by the rigid support rod. Global adjustments were made to brightness, contrast, and gamma, within the Photron software (PFV). Additional level adjustments were made to highlight the smoke lines using Photoshop with a mask over the flower, shown in green.

Inertial power comparisons quantitatively confirm consistency of flower wake and reveal nonlinearity

To test if flower tracking in wind (case 1) is a linear superposition of stationary hovering in wind (case 2, Fig. 6A,B) and tracking in still air (case 3), we sought to compare the mechanical power utilized during these three different conditions. For the two tracking cases, (1) and (3), moths exhibit inertial power peaks at each of the driving frequencies and minimal power at the non-driving frequencies (Fig. 6C). When the flower is held stationary in wind (case 2), we expect that power requirements should only increase in the frequency band corresponding to vortex shedding. A stationary flower would result in a stationary moth and therefore low inertial COM power. Then, inertial COM power for hover-feeding in wind (case 2) reveals the maneuvers induced by flower

wake interactions (Fig. 6D). The sum of the moth's inertial power for hover-feeding in wind (case 2) and tracking in still air (case 3), give a linear prediction for the power needed to track in wind (case 1).

$$\widehat{\dot{E}}^{wind}_{tracking} = \dot{E}^{still}_{tracking} + \dot{E}^{wind}_{hovering}. \tag{7}$$

The linear sum over-predicts the measured response for tracking in wind at all non-driving frequencies (Fig. 6E). The response at the lowest driving frequencies is well-captured by a linear combination of still air tracking and hover-feeding in wind. However, at the mid-range driving frequencies (1.7-5.3 Hz), the linear sum consistently under-predicts the actual response by a minimum of 11.4 W kg^{-1} (at 5.3 Hz) and a maximum of 92.1 W kg^{-1} (at 2.9 Hz). Although there is a slight increase in inertial power between hover-feeding (case 2) and tracking in wind (case 3), the over-prediction by the linear sum, especially between 2-5 Hz (Fig. 6E), is too large to be explained by differences in flower wake characteristics alone.

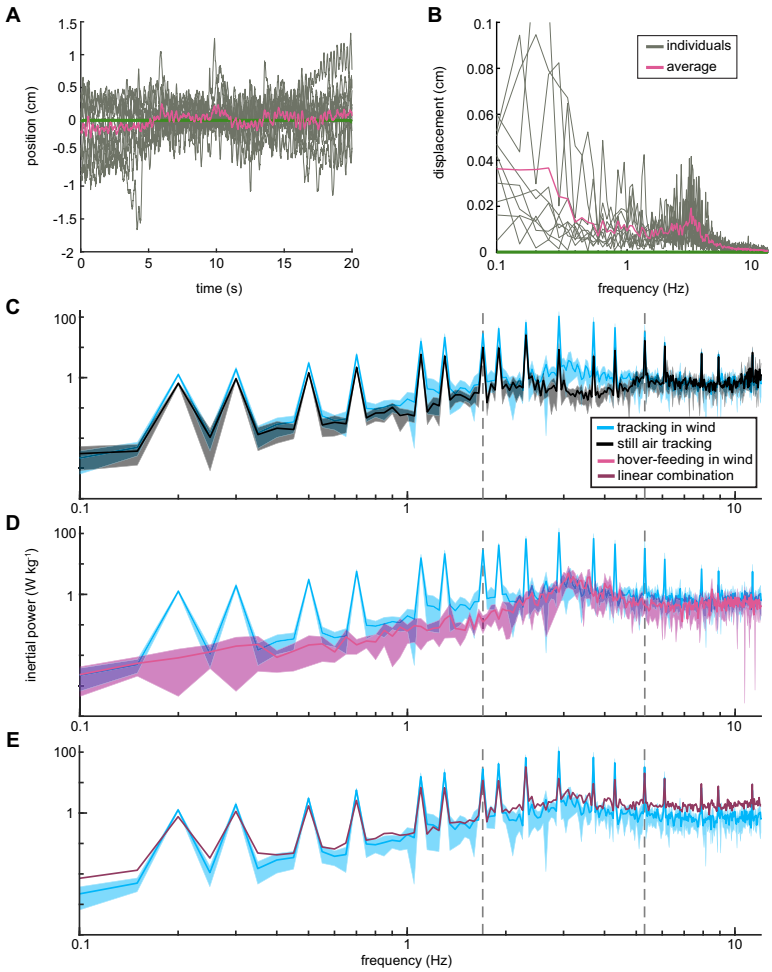

Fig. 6. Effects of unsteady wake on inertial power. (A) Example time series data for hover-feeding trials in the wind tunnel. The flower (green) remains stationary while the moth oscillates and tries to maintain a stable position with 0.7 m s^{-1} freestream wind. Traces showing trajectories of all sampled moths (grey) and the mean (pink) show high variation between individuals. (B) Fourier transform of data (from A). Each individual trial was transformed and then averaged. Despite individual variation, all moths display large amplitude oscillations below 1.7 Hz with an additional (smaller) peak occurring between 2-5 Hz. (C) Inertial (COM) power comparison for tracking in wind (blue) and in still air (black). Power peaks at the driving frequencies for both tracking cases, but peaks are higher for tracking in wind. (D) Comparison for tracking in wind (blue) and hover-feeding in wind (pink). Power peaks at the driving frequencies for tracking in wind, but both traces show agreement in non-driving frequencies between 1.7-5.3 Hz. (E) Comparison between measured tracking in wind (blue) and the linear combination of still air tracking (Sponberg et al (2015)) and hover-feeding in wind (dark purple). While the linear combination agrees fairly well with the response at the lowest frequencies, it under-predicts the response between 1.7-5.3 Hz and over-predicts at the highest frequencies.

Key features of the leading edge vortex are maintained in wind

The discrepancy between predicted and measured tracking in wind indicates that flower wake interactions do influence tracking maneuvers. We next used smoke visualization to see if the leading edge vortex persists in wind and maintains the same structural features while the wings interact with the flower wake. The vortex structure in steady air shows a relatively constant diameter at mid-wing and over the thorax, with a continuous vortex connecting the two (Bomphrey et al. 2005).

However, the leading edge vortex in wind retains the same structure over the wings and thorax that was seen with previous smoke visualization in steady air conditions (Ellington et al. 1996, Bomphrey et al. 2005). The mid-wing LEV protrudes beyond the extent of the flower face (Fig. 7A), and grows from the start of the downstroke until it is shed prior to the beginning of the

upstroke. The LEV is most visible at mid-downstroke (Fig. 7A and Movie S2). Although the free-stream velocity in our experiments was slightly lower than in previous studies (Ellington et al. 1996, Bomphrey et al. 2005), the LEV at the mid-wing position is qualitatively similar in size (relative to the wing chord) and shape to their results. Other features of the LEV structure, such as trailing edge (Fig. 7B, white arrow) and tip vortices (Fig. 7A, yellow arrow) are also visible on some wingstrokes, but the full vortex loop structure cannot be resolved with smoke-wire visualization.

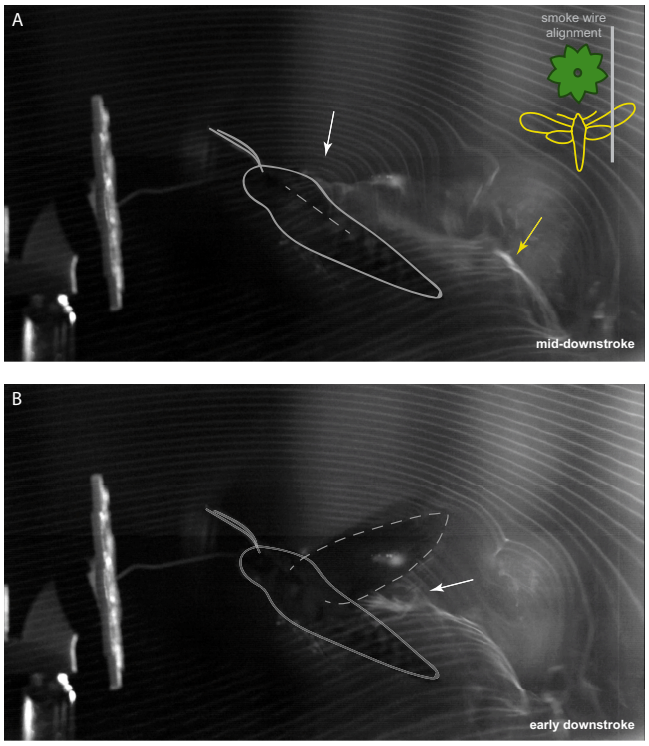

Fig. 7. Smoke visualization of the leading edge vortex at the mid-wing position. Free-flying moths maintaining a stable position while feeding from the robotic flower in wind. Outline of moth added for clarity. (A) Mid-downstroke. Separated flow region of LEV (white arrow) and roll up of the tip vortex (yellow arrow). The LEV during the mid to late downstroke resembles what has been seen previously for tethered *Manduca* in steady air (compare to Bomphrey et al (2006)), but the tip vortex (yellow arrow) shows a down and backward trajectory, rather than back and upwards. (B) Early downstroke. A possible trailing edge vortex (TEV) indicated by a white arrow. Level adjustments were made to highlight the smoke lines using Photoshop. Inset shows smoke wire lateral alignment with the moth and flower face.

In addition to sustaining the LEV at mid-wing throughout the wingstroke, smoke visualization of flow over the thorax showed that the moth still maintains a connected LEV structure across the full wingspan. As in steady flight (Bomphrey et al. 2005), the thorax-spanning LEV forms during stroke reversal and grows during the upstroke (Fig. 8B and Movie S3). The LEV over the thorax is approximately the same size and structure as the LEV seen at mid-wing (compare to Fig. 7A). However, a transient LEV was sometimes present during the downstroke (Fig. 8A), so LEV structure may not be conserved from from wingbeat to wingbeat. Despite possible inter-wingbeat variation, moths appear to use the same LEV to generate lift with and without wind.

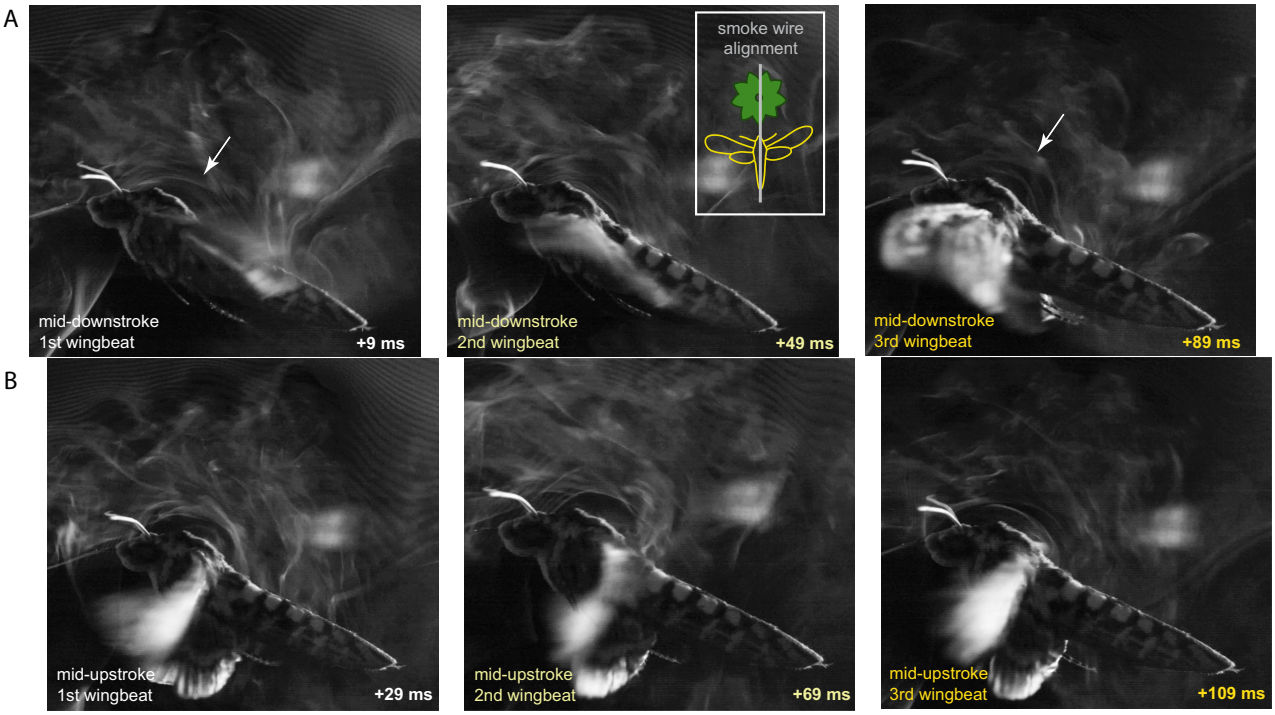

Fig. 8. Smoke visualization of the leading edge vortex over the thorax (centerline). Flow is attached over the thorax at the late downstroke (for most wingstrokes), separates at stroke reversal, and then the LEV grows throughout the upstroke. Snapshots from three successive wingbeats show (A) a transient downstroke LEV over the thorax and (B) the persistent thorax LEV at mid-upstroke. Relative time throughout each wingbeat is shown based on the approximately 24 Hz (or 40 ms) wingbeat frequency (Fig. S2). When present (white arrow), the downstroke LEV is comparable in size to the upstroke LEV. Inset shows smoke wire lateral alignment with the moth and flower.

Discussion

Wake interactions shift tracking performance within vortex shedding frequency range

We discovered that wind affects moth maneuverability, but only at the specific frequencies that vortices are shed in the flower wake. Although performance is slightly lower, moths maintain near perfect tracking in the flower wake within the range of flower oscillations they encounter in nature. Outside of this range, moths face significant challenges from vortices shed in the flower wake. Gain overshoot, tracking error, and inertial power, all peak within 2-5 Hz and are higher than in still air (Figs. 3D,F and 6C,D,E). Hawkmoths (Ortega-Jimenez et al. 2013), bumblebees (Ravi et al. 2013), and fish (Liao et al. 2003*b*,*a*, Liao 2007, Maia et al. 2015) have all demonstrated an ability to stabilize perturbations at vortex shedding frequencies when maintaining a position. We found that shed vortices also impact active maneuvers, like flower tracking, but tracking maneuvers at biologically relevant frequencies show little change compared to still air.

It is surprising that responses to the flower wake are consistent across all non-driving frequencies, regardless of whether the flower is moving or not. Wakes of oscillating cylinders exhibit increased vortex strength (Toebes 1969) and varied modes of vortex shedding depending on the frequency of oscillation (Griffin 1971, Williamson & Roshko 1988, Placzek et al. 2009). When the cylinder oscillates at the natural vortex shedding frequency of the still cylinder, a "lock-in" condition can be

reached where the motion of the cylinder can drive vortex shedding away from the natural frequency (Koopmann 1967). Although the mean inertial power for moving and still flowers in wind differs slightly at non-driving frequencies outside of the vortex shedding range, the confidence intervals maintain overlap (Fig. 6D). The consistent overlap across non-driving frequencies in wind suggests that the vortex shedding in the flower wake occurs between 2-5 Hz whether the flower is moving or not (Fig. 6D). Separation between vortex shedding frequencies and flower motion frequencies may allow the moth to decouple tracking maneuvers and perturbation responses.

In nature, even wind speeds below 5 cm s^{-1} induce small amplitude oscillations (approximately 0.5 cm, peak-to-peak) in hawkmoth pollinated flowers (*Phlox*) and higher wind speeds result in larger lateral than longitudinal oscillations (Farina et al. 1994). Frequency analysis of multiple flower species showed that most hawkmoth-pollinated flowers oscillate below 5 Hz (Sprayberry & Suver 2011) with over 90% of flower power (power spectral density or oscillation energy at each frequency) contained below 1.7 Hz (Sponberg et al. 2015). In addition to oscillating within this low frequency band (0.1-1.7 Hz), we found that natural hawkmoth-pollinated flowers shed wake structures at these frequencies (Fig. 5). Because the frequencies of flower oscillation and vortex shedding overlap, flower wakes could pose challenges to tracking in nature. Alternatively, if the passive response to wind is in the same direction as tracking motion, then moths could exploit this phenomenon to "surf" on flower wakes.

Interplay between tracking and interacting with wind leads to a nonlinear inertial power response

The nonlinear inertial power for tracking in wind means that there is a more complicated interaction of airflow and maneuvers than a simple superposition. More motion than predicted is seen at the driving frequencies, especially at frequencies (2-5 Hz) where the flower sheds vortices (Figs. 4 and 6). When tracking error increases above 1 ($\epsilon > 1$), the moth no longer benefits from tracking maneuvers and would better match flower motion if it simply hovered in place. The moth cannot independently control for each frequency while tracking. Importantly, if the moth attempted to reduce gain at higher frequencies, tracking performance at the lower natural flower motion frequencies would suffer. Between 1.7-5.3 Hz tracking error is greater than 1 with and without wind, but more than doubles with wind (Fig. 3F). However, tracking performance is reduced in the flower wake, with a larger effect at vortex shedding frequencies. This suggests that tracking dynamics may be tuned to facilitate tracking maneuvers at frequencies that match natural flower oscillations. Then, the addition of unsteady flow emphasizes that best tracking performance is biased to these low frequencies.

Below 1.7 Hz wind seems to not affect body motion, so the moth always benefits from tracking maneuvers and tracking error remains below one. Moths are potentially perturbed by wind, but if so, they may be correcting for this through feedback. Both experiments and numerical simulations showed that bumblebees in von Kármán streets respond to perturbations with passive, drag-based mechanisms (Hedrick et al. 2009, Ristroph et al. 2013), but must also use active flight control to

maintain stability as wake perturbation effects increase over time (Ravi et al. 2016). In addition, we know the abdomen responds actively to visual motion stimuli to stabilize body pitch over multiple wingstrokes (Dyhr et al. 2013). Hawkmoths maneuvering in wind could adjust abdomen position either to increase drag and stabilize against perturbations or tilt their aerodynamic force vector without changing wing kinematics.

Measurements of energetic costs of tracking showed that maneuvering does increase costs, but the increase is small compared to the energy required for hovering alone (Sprayberry & Daniel 2007). Although the flower wake could increase the energy needed to hover, increased inertial power requirements for motion may not be accompanied by increased power output (or metabolic) demands. Rainbow trout adopt a Kármán gait to slalom though unsteady wakes and reduce costs of locomotion (Liao et al. 2003*a*). Moths could use the energy in the wake to track the flower by tuning the timescale of the wingbeat to enhance lift (Lehmann 2008, Lua et al. 2011, 2017). If so, they may not need to control against perturbations occurring at the driving frequencies, even if this results in increased overshoot (Fig. 3D). The increased overshoot at vortex shedding frequencies implies that wake structures interact aerodynamically with the moth to transfer momentum which challenges our assumption of constant aerodynamic forces for hovering. Fluctuations in aerodynamic power requirements could be indicated by changes in known aerodynamic mechanisms, such as LEV formation and stability.

LEV seen in steady air persists despite unsteady wake interactions

In wind, the flower sheds vortices in multiple directions causing multidirectional flow separation at the leading edge of the wing, which may inhibit the ability of each wing to generate bound vortices, such as the LEV. To maintain LEV structure and size, energy must be dissipated or the vortex would continue to grow in size and strength until it is shed off of the wing into the wake of the insect. Interaction with vortices in the flower wake could contribute additional energy that would also need to be dissipated, potentially leading to changes in spanwise flow along the wing (Birch & Dickinson 2001). Visualizing structural changes in the LEV while the moth hovers in the flower wake reveals whether moths alter their aerodynamic lift mechanism in wind. Although the flower wake is energetic enough to disrupt tracking, LEV structure in the wake is qualitatively the same as in steady air. Therefore, additional energy from the flower wake is successfully dissipated out of the LEV. Quantitative visualization of flow along the wingspan could show if this energy transported through the LEV core, potentially changing lift production.

We see no evidence of vortex bursting due to interaction with the flower wake, even though LEVs can burst at Reynolds numbers relevant for hawkmoth flight (Re>1400) (Lentink & Dickinson 2009). Therefore, we conclude that the leading edge vortex is robust to interactions with vortex structures at the spatiotemporal scale of the robotic flower. Stability of the LEV in wind could be due to the small size of vortex structures (Fig. 4), suggesting they may not be energetic enough to cause disruption. The comparable size of vortices in natural flower wakes (Fig. 5) also implies that vortex size is not a challenge to the LEV in nature. The temporal range of vortex shedding frequencies (2-5

Hz) lies well below the wingbeat frequency of the moth during hovering and tracking (approximately 25 Hz). We found that while interacting with wind at these frequencies moths still maintain the timescale of the wingbeat (Fig. S3). Therefore the timescale of LEV growth is also maintained in the unsteady flower wake. Quantitative flow visualization of LEV strength and development throughout the wingstroke could reveal if lift forces are affected by interactions with wind although the LEV structure appears not to change.

Distinct categories of LEVs have been identified for many different insects. Each category describes a specific class of LEV based on the qualitative structure of the vortex across the wingspan and a quantitative understanding of how energy is dissipated to maintain LEV stability (Bomphrey et al. 2005). Identification of structural properties of the flow at critical points along the wingspan found that hawkmoths rely on a continuous, actively generated LEV in steady air (Willmott et al. 1997). Our results show that moths continue to use the same aerodynamic lift mechanism in wind. Visualization of flow over both the centerline (Fig. 8) and mid-wing position (Fig. 7) confirms the same qualitative LEV structure, position, and size throughout the wingstroke and across multiple wingbeats.

Counterintuitive reduced-order dynamics emerge in a more complex environment

Maintaining a stable LEV could cause moths to simplify their motion during complex body maneuvers in wind. Despite the nonlinear increase in inertial power, moths produce reduced-order dynamics for tracking in wind, compared to still air. Interaction with the flower wake removes the bimodal response in both gain and phase within the range of vortex shedding frequencies (Fig. 3D,E). This suggests that the flower wake acts as an environmental bandpass filter to simplify tracking dynamics within 2-5 Hz. With and without wind, performance is best at low frequencies and drops as frequency increases (Fig. 3D,E), showing that the same underlying tracking dynamics are at play. Electric fish tracking refuges exhibit similar dynamics peaked around frequencies <1 Hz implying a high-pass controller for motion based on forces impacting the animal (Cowan & Fortune 2007). Similar inertial and added mass effects influence tracking hawkmoths with potentially even larger consequences an unsteady wake. The high-pass controller for tracking may only be needed to respond to high frequency perturbations. *Eigenmannia* also varies opposing thrust and drag forces to remain stable in different flow speeds (Sefati et al. 2013). Passive responses to vortices in the flower wake could counteract higher-order tracking maneuvers at certain frequencies, even if the moth does not deliberately control against these perturbations. Then, performance at natural flower frequencies may be conserved across environments.

Since multiple hawkmoth species rely on the same flight mechanics to track flowers, they should respond similarly to the same flower wake. However, morphological differences in mass and wingspan may influence the magnitude of the effect of wind on tracking and the LEV. In still air, flower tracking dynamics for hawkmoths *M. sexta*, *D. elpenor*, and *M. stellatarum* can all be described by a minimum third-order, delayed transfer function (Stöckl et al. 2017) despite inter-species differences. The minimum order is largely due to the plateau in the phase response (Fig. 3E), which is also

seen in crepuscular *D. elpenor* and diurnal *M. stellatarum*. Given that *M. sexta* is much larger than the other two species (at least twice as massive with a 60%-250% larger wingspan (Henningsson & Bomphrey 2013)), they may be more able to maintain tracking performance than the smaller moths. The larger *M. sexta* would also need to generate more lift (per unit mass), potentially emphasizing the need for LEV stability. Therefore, moths may simplify tracking dynamics in wind to maintain control over aerodynamic forces and, minimally, continue to hover and feed from the flower.

Contradiction in wake impact on maneuvering and aerodynamics

Hawkmoths employ the same leading edge vortex to produce lift despite changing how well track flowers in still and windy conditions. Since vortices in the flower wake are relatively small, interactions between these structures and the LEV may result in vorticity or lift magnitude differences, but not cause the overall LEV structure to change along the wingspan. Critical features of the LEV over the wings (Fig. 7) and thorax (Fig. 8) demonstrate that the same class of LEV is effective in unsteady and steady flow (Bomphrey et al. 2005). While smoke visualization identifies the presence of the LEV, it cannot resolve changes in spanwise flow, either through the vortex core or towards the trailing edge of the wing. We conclude that any changes in spanwise flow due to the flower wake are small enough to not change LEV class. We plan to validate this in the future by quantifying the full 3D LEV structure with tomographic PIV.

Insects could use a variety of flight control mechanisms to change their tracking dynamics while maintaining LEV stability. Hawkmoths perform sideslips to track and mitigate perturbations by re-orienting their force vector through coupling between rotational and translational motions (Greeter & Hedrick 2016). Since the leading edge vortex remains stable for hawkmoths in the flower wake, it could be used to help the animal maneuver through re-orientation of the lift force vector. Behavior in nature combines controlled maneuvers through an unsteady environment that can dynamically interact with the animal to disrupt locomotion (Watkins et al. 2006, Kolomenskiy et al. 2016). Although tracking maneuvers are simplified, the mechanism for generating the forces necessary for motion, such as lift during flight, appears robust to the windy environment (Figs. 7 and 8).

Consequences for flight control

Freely behaving animals rely on feedback systems to control locomotion and encode information about both the environment and their state within that environment. Fish swimming through von Kármán cylinder wakes largely maintain position through visual feedback (Liao 2007). The foraging task studied here was previously shown to rely on redundant visual and mechanosensory (from the proboscis-nectary interaction) pathways (Roth et al. 2016). The addition of mechanical feedback may help moths stabilize in wakes even if their vision is compromised. *M. sexta* also has a longer proboscis than other hawkmoths, *D. elpenor* or *M. stellatarum* (Haverkamp et al. 2016), which has been proposed to increase mechanical feedback during tracking since more of the proboscis is in contact with the nectary (Stöckl et al. 2017). A longer proboscis could also cause the moth to interact with vortices that develop further downstream from the flower, requiring the LEV to also

be stable to the wakes of a wide range of flowers from *Petunia* to larger *Datura* (Fig. 5).

As they maneuver in nature, insects may need to encode both the environment around them and the forces they are able to produce through interactions with that environment. Campaniform sensilla present along the dorsal and ventral side of the the hawkmoth forewing are sensitive to inertial forces on a timescale 80x smaller than the wingbeat period (Dickerson et al. 2014, Pratt et al. 2017). While these studies measured body forces, motion may also be encoded along the wing itself by detecting changes in forces, such as fluctuating rotational accelerations. LEV stability is maintained across biological systems based on the Coriolis and centripetal accelerations acting on the wing (Lentink & Dickinson 2009, Chin & Lentink 2016). Given their potential sensitivity to Coriolis forces, it is possible that insects use the array of sensilla on their wings to not only sense changes in the environment, but also changes to rotational accelerations acting along the wing that could destabilize the LEV. The sensilla may also be used to sense changes in flow within the LEV that could lead to disruptions of LEV integrity. Detecting changes to LEV stability could be a mechanical feedback mechanism for moths to keep hovering and feeding even when sensors on the proboscis are compromised.

Although performance suffers, the forces and torques fundamental to successful flower tracking at natural flower oscillation frequencies are maintained in wind. Features of the environment are sensed and integrated by multiple neural pathways to achieve a desired motion. Variation in the environment then shifts behavior away from ideal locomotion, but not far enough to cause failure. Animals in nature may depend on sensing subtle changes in force-generating mechanisms, such as the LEV, to balance body maneuvers and lift production in an unsteady environment.

Acknowledgements

We thank Steven Chandler for his assistance in setting up and maintaining the animals and experimental apparatus and many thoughtful discussions of the frequency domain. We also thank Isabel Veith for preparing supplementary information about the wind tunnel specifications.

Competing interests

The authors declare no competing or financial interests.

Author Contributions

Conceptualization, methodology, resources, writing – review and editing, and funding acquisition: M.G.M. and S.N.S.; Software, validation, formal analysis, investigation, data curation, visualization, and writing – original draft and preparation: M.G.M.; Supervision: S.N.S.

Funding

This work was supported by a National Science Foundation Graduate Research Fellowship (NSF GRFP), [Grant No. DGE-1650044 to M.G.M.] and an NSF Physics of Living Systems Career Grant

[Grant No. MPS/PoLS 1554790 to S.N.S.].

References

Birch, J. M. & Dickinson, M. H. (2001), 'Spanwise flow and the attachment of the leading-edge vortex on insect wings', *Nature* **412**, 729–733.

Bomphrey, R. J., Lawson, N. J., Harding, N. J., Taylor, G. K. & Thomas, A. L. R. (2005), 'The aerodynamics of Manduca sexta: digital particle image velocimetry analysis of the leading-edge vortex', *Journal of Experimental Biology* **208**, 1079–1094.

Bomphrey, R. J., Taylor, G. K. & Thomas, A. L. R. (2009), 'Smoke visualization of free-flying bumblebees indicates independent leading-edge vortices on each wing pair', *Experiments in Fluids Fluids* **46**, 811–821.

Broadhead, G. T., Basu, T., von Arx, M. & Raguso, R. A. (2017), 'Diel rhythms and sex differences in the locomotor activity of hawkmoths', *Journal of Experimental Biology* pp. 1472–1480.

Chin, D. D. & Lentink, D. (2016), 'Flapping wing aerodynamics: from insects to vertebrates', *Journal of Experimental Biology* **219**, 920–932.

Combes, S. A. & Dudley, R. (2009), 'Turbulence-driven instabilities limit insect flight performance', *Proceedings of the National Academy of Sciences* **106**(22), 9105–9108.

Cowan, N. J. & Fortune, E. S. (2007), 'The critical role of locomotion dynamics in decoding sensory systems', *J. Neurosci.* **27**(5), 1123–1128.

Dickerson, B. H., Aldworth, Z. N. & Daniel, T. L. (2014), 'Control of moth flight posture is mediated by wing mechanosensory feedback', *Journal of Experimental Biology* **217**, 2301–2308.

Dudley, R. (2002*a*), 'Mechanisms and Implications of Animal Flight Maneuverability', *Integrative and Comparative Biology* **42**, 135–140.

Dudley, R. (2002*b*), *The Biomechanics of Insect Flight: Form, Function, Evolution*, Princeton.

Dyhr, J. P., Morgansen, K. A., Daniel, T. L. & Cowan, N. J. (2013), 'Flexible strategies for flight control: an active role for the abdomen', *Journal of Experimental Biology* **216**, 1523–1536.

Ellington, C. P., van den Berg, C., Willmott, A. P. & Thomas, A. R. (1996), 'Leading-edge vortices in insect flight', *Nature* **384**, 626–630.

Farina, W. M., Kramer, D. & Varjú, D. (1995), 'The response of the hovering hawk moth Macroglossum stellatarum to translatory pattern motion', *Journal of Comparative Physiology A* **176**, 551–562.

Farina, W. M., Varjú, D. & Zhou, Y. (1994), 'The regulation of distance to dummy flowers during hovering flight in the hawk moth Macroglossum stellatarum', *Journal of Comparative Physiology A* **174**, 239–247.

Greeter, J. S. M. & Hedrick, T. L. (2016), 'Direct lateral maneuvers in hawkmoths', *Biology Open* pp. 1–11.

Griffin, O. M. (1971), 'The Unsteady Wake of an Oscillating Cylinder at Low Reynolds Number', *Journal of Applied Mechanics* **38**, 729.

Haverkamp, A., Bing, J., Badeke, E., Hansson, B. & Knaden, M. (2016), 'Innate olfactory preferences for flowers matching proboscis length ensure optimal energy gain in a hawkmoth', *Nature Communications* **7**, 1–9.

Hedrick, T. L. (2008), 'Software techniques for two- and three-dimensional kinematic measurements of biological and biomimetic systems', *Bioinspiration & Biomimetics* **3**.

Hedrick, T. L., Cheng, B. & Deng, X. (2009), 'Wingbeat Time and the Scaling of Passive Rotational Damping in Flapping Flight', *Science* **324**, 252–255.

Henningsson, P. & Bomphrey, R. J. (2013), 'Span efficiency in hawkmoths', *Journal of the Royal Society Interface* **10**, 20130099.

Kolomenskiy, D., Ravi, S., Takabayashi, T., Ikeda, T., Ueyama, K., Engels, T., Fisher, A., Tanaka, H., Schneider, K., Sesterhenn, J. & Liu, H. (2016), 'Added costs of insect-scale flapping flight in unsteady airflows', *arXiv preprint* pp. 1–15.

Koopmann, G. H. (1967), 'The vortex wakes of vibrating cylinders at low Reynolds numbers', *J. Fluid Mech.* **28**, 501–512.

Lehmann, F.-O. (2008), 'When wings touch wakes: understanding locomotor force control by wake wing interference in insect wings', *Journal of Experimental Biology* **211**(2), 224–233.

Lentink, D. & Dickinson, M. H. (2009), 'Rotational accelerations stabilize leading edge vortices on revolving fly wings', *Journal of Experimental Biology* **212**, 2705–2719.

Lentink, D., Van Heijst, G. F., Muijres, F. T. & Van Leeuwen, J. L. (2010), 'Vortex interactions with flapping wings and fins can be unpredictable', *Biology Letters* **6**(3), 394–397.

Liao, J. C. (2007), 'A review of fish swimming mechanics and behaviour in altered flows', *Philosophical Transactions of the Royal Society B: Biological Sciences* **362**, 1973–1993.

Liao, J. C., Beal, D. N., Lauder, G. V. & Triantafyllou, M. S. (2003*a*), 'Fish Exploiting Vortices Decrease Muscle Activity', *Science* **302**, 1566–1569.

Liao, J. C., Beal, D. N., Lauder, G. V. & Triantafyllou, M. S. (2003*b*), 'The Kármán gait: novel body kinematics of rainbow trout swimming in a vortex street', *Journal of Experimental Biology* **206**, 1059–1073.

Lighthill, M. J. (1973), 'On the Weis-Fogh mechanism of lift generation', *Journal of Fluid Mechanics* **60**, 1–17.

Lua, K. B., Lee, Y. J., Lim, T. T. & Yeo, K. S. (2017), 'WingâĂŞWake Interaction of Three-Dimensional Flapping Wings', *AIAA Journal* **55**(3), 729–739.

Lua, K. B., Lim, T. T. & Yeo, K. S. (2011), 'Effect of wing-wake interaction on aerodynamic force generation on a 2D flapping wing', *Experiments in Fluids* **51**, 177–195.

Maia, A., Sheltzer, A. P. & Tytell, E. D. (2015), 'Streamwise vortices destabilize swimming bluegill sunfish (Lepomis macrochirus)', *Journal of Experimental Biology* **218**, 786–792.

Merzkirch, W. (1987), Techniques of Flow Visualization, Technical report, Advisory Group for Aerospace Research & Development.

Ortega-Jimenez, V. M., Badger, M., Wang, H. & Dudley, R. (2016), 'Into rude air: hummingbird flight performance in variable aerial environments', *Philosophical Transactions of the Royal Society of London B: Biological Sciences* **371**(1704), 20150387.

Ortega-Jimenez, V. M., Greeter, J. S. M., Mittal, R. & Hedrick, T. L. (2013), 'Hawkmoth flight stability in turbulent vortex streets', *Journal of Experimental Biology* **216**, 4567–4579.

Ortega-Jimenez, V. M., Mittal, R. & Hedrick, T. L. (2014), 'Hawkmoth flight performance in tornado-like whirlwind vortices', *Bioinspiration & Biomimetics* **9**.

Placzek, A., Sigrist, J. F. & Hamdouni, A. (2009), 'Numerical simulation of an oscillating cylinder in a cross-flow at low Reynolds number: Forced and free oscillations', *Computers and Fluids* **38**, 80–100.

Pournazeri, S., Segre, P. S., Princevac, M. & Altshuler, D. L. (2013), 'Hummingbirds generate bilateral vortex loops during hovering: Evidence from flow visualization', *Experiments in Fluids* **54**(1).

Pratt, B., Deora, T., Mohren, T. & Daniel, T. L. (2017), 'Neural evidence supports a dual sensory-motor role for insect wings', *Proceedings of the Royal Society B: Biological Sciences* **284**.

Ravi, S., Crall, J. D., Fisher, A. & Combes, S. A. (2013), 'Rolling with the flow: bumblebees flying in unsteady wakes', *Journal of Experimental Biology* **216**, 4299–4309.

Ravi, S., Crall, J. D., McNeilly, L., Gagliardi, S. F., Biewener, A. A. & Combes, S. A. (2015), 'Hummingbird flight stability and control in freestream turbulent winds', *Journal of Experimental Biology* **218**, 1444–1452.

Ravi, S., Kolomenskiy, D., Engels, T., Schneider, K., Wang, C., Sesterhenn, J. & Liu, H. (2016), 'Bumblebees minimize control challenges by combining active and passive modes in unsteady winds', *Scientific Reports* **6**.

Riffell, J. A., Shlizerman, E., Sanders, E., Abrell, L., Medina, B., Hinterwirth, A. J. & Kutz, J. N. (2014), 'Flower discrimination by pollinators in a dynamic chemical environment', *Science* **344**(6191), 1515–1518.

Ristroph, L., Ristroph, G., Morozova, S., Bergou, A. J., Chang, S., Guckenheimer, J., Wang, Z. J. & Cohen, I. (2013), 'Active and passive stabilization of body pitch in insect flight', *Journal of the Royal Society Interface* **10**.

Roth, E., Hall, R. W., Daniel, T. L. & Sponberg, S. (2016), 'Integration of parallel mechanosensory and visual pathways resolved through sensory conflict', *Proceedings of the National Academy of Sciences* **113**(45), 12832–12837.

Roth, E., Sponberg, S. & Cowan, N. J. (2014), 'A comparative approach to closed-loop computation', *Current Opinion in Neurobiology* **25**, 54–62.

Roth, E., Zhuang, K., Stamper, S. A., Fortune, E. S. & Cowan, N. J. (2011), 'Stimulus predictability mediates a switch in locomotor smooth pursuit performance for Eigenmannia virescens', *Journal of Experimental Biology* **214**, 1170–1180.

Sane, S. P. (2003), 'The aerodynamics of insect flight', *Journal of Experimental Biology* **206**, 4191–4208.

Sefati, S., Neveln, I. D., Roth, E., Mitchell, T. R. T., Snyder, J. B., MacIver, M. A., Fortune, E. S. & Cowan, N. J. (2013), 'Mutually opposing forces during locomotion can eliminate the tradeoff between maneuverability and stability', *Proceedings of the National Academy of Sciences* **110**(47), 18798–18803.

Sponberg, S. & Daniel, T. L. (2012), 'Abdicating power for control: a precision timing strategy to modulate function of flight power muscles', *Proceedings of the Royal Society B: Biological Sciences* **279**, 3958–3966.

Sponberg, S., Dyhr, J. P., Hall, R. W. & Daniel, T. L. (2015), 'Luminance-dependent visual processing enables moth flight in low light', *Science* **348**, 1245–1248.

Sprayberry, J. D. H. & Daniel, T. L. (2007), 'Flower tracking in hawkmoths: behavior and energetics', *Journal of Experimental Biology* **210**, 37–45.

Sprayberry, J. D. H. & Suver, M. (2011), 'Hawkmoths' innate flower preferences: A potential selective force on floral biomechanics', *Arthropod-Plant Interactions* **5**, 263–268.

Srygley, R. B. & Thomas, A. L. R. (2002), 'Unconventional lift-generating mechanisms in free-flying butterflies', *Nature* **420**, 660–664.

Stöckl, A. L., Kihlstrom, K., Chandler, S. & Sponberg, S. (2017), 'Comparative system identification of flower tracking performance in three hawkmoth species reveals adaptations for dim light vision', *Philosophical Transactions of the Royal Society B: Biological Sciences* **372**.

Theobald, J. C., Warrant, E. J. & O'Carroll, D. C. (2009), 'Wide-field motion tuning in nocturnal hawkmoths.', *Proceedings of the Royal Society B: Biological Sciences* **277**, 853–860.

Toebes, G. H. (1969), 'The unsteady flow and wake near an oscillating cylinder', *Journal of Basic Engineering* **91**, 493–502.

Watkins, S., Milbank, J., Loxton, B. J. & Melbourne, W. H. (2006), 'Atmospheric winds and their implications for microair vehicles', *AIAA Journal* **44**(11), 2591–2600.

Weis-Fogh, T. (1973), 'Quick Estimates of Flight Fitness in Hovering Animals, Including Novel Mechanisms for Lift Production', *Journal of Experimental Biology* **59**, 169–230.

Williamson, C. H. K. & Roshko, A. (1988), 'Vortex formation in the wake of an oscillating cylinder', *Journal of Fluids and Structures* **2**, 355–381.

Willmott, A. P. & Ellington, C. P. (1997*a*), 'Measuring the angle of attack of beating insect wings: robust three-dimensional reconstruction from two-dimensional images', *Journal of Experimental Biology* **200**, 2693–704.

Willmott, A. P. & Ellington, C. P. (1997*b*), 'The mechanics of flight in the hawkmoth Manduca sexta. I. Kinematics of hovering and forward flight', *Journal of Experimental Biology* **200**, 2723–2745.

Willmott, A. P. & Ellington, C. P. (1997*c*), 'The mechanics of flight in the hawkmoth Manduca sexta. II. Aerodynamic consequences of kinematic and morpholocial variation', *Journal of Experimental Biology* **200**, 2723–2745.

Willmott, A. P., Ellington, C. P. & Thomas, A. L. R. (1997), 'Flow visualization and unsteady aerodynamics in the flight of the hawkmoth, Manduca sexta', *Philosophical Transactions of the Royal Society B: Biological Sciences* **352**, 303–316.